

# In-Situ Neutron Diffraction Study of the Austenite to Ferrite Transformation during Deformation at Temperatures at and above the Upper Critical Temperature

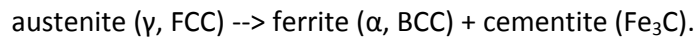
Chiradeep Ghosh<sup>1</sup> and Michael Gharghour<sup>2</sup>

<sup>1</sup> Materials Engineering, McGill University, Montreal, QC, Canada

<sup>2</sup> NRC Canadian Neutron Beam Centre, Chalk River Laboratories, Chalk River, ON, Canada

## BACKGROUND

After solidification, a steel remains completely austenitic until its temperature falls to the  $Ae_3$ , or *upper critical temperature* line. As it cools below the  $Ae_3$ , the iron begins to change from its face centered cubic (FCC, austenite,  $\gamma$ ) form to its body centered cubic (BCC, ferrite,  $\alpha$ ) form. Small crystals of ferrite begin to separate out from the austenite. The ferrite crystals retain a small amount of carbon (less than 0.03%). As cooling proceeds, the ferrite grows at the expense of the austenite. By the time the steel has reached the  $Ae_1$  line at 723°C (called the lower critical temperature), it is composed of ferrite and austenite. At this stage the austenite contains 0.8% carbon. Austenite cannot normally hold more than 0.8% carbon in solid solution at 723°C. As the temperature drops further, the remaining austenite undergoes the eutectoid reaction, forming a mixture of ferrite and cementite.



The equilibrium Fe-C phase diagram shows the phase changes that occur during slow heating and cooling and the nature and amount of the phases that exist at any temperature. These diagrams are widely known and of considerable utility. The characteristics of non-equilibrium Fe-C phase diagrams are not fully known at the moment. For example, T-T-T (Time-Temperature-Transformation) diagrams depict the relationships between phases, temperature and time. These diagrams are relevant to cooling behavior only. The goal of the present project is to determine a non-equilibrium phase diagram during deformation at high temperature.

In the 1980's, Yada and co-workers [1,2] succeeded in transforming austenite into ferrite at temperatures above the  $Ae_3$  as long as the former was undergoing deformation. They investigated the behavior of two low-C steels, with  $Ae_3$  temperatures of 838 and 834°C, which were subjected to deformation at 900°C, i.e. about 65°C above the equilibrium transformation temperature. They produced ferrite grains 1 to 2 nm in size, as long as a critical strain of about 0.5 was exceeded, and observed that the ferrite volume fraction increased with deformation from about 5% at the critical strain to about 70 to 80% at strains of 3 to 4. They also reported that, on holding at temperature after deformation, the reverse transformation took place i.e., the newly formed ferrite transformed back into austenite.

In 2004, Tong *et al.* [3] used Monte Carlo methods to model the formation of ferrite from austenite above the  $A_{e3}$ , as well as the reverse ferrite-austenite transformation. This model was later extended by Xiao *et al.*, [4] who allowed for the occurrence of dynamic recrystallization (DRX) as well as dynamic transformation (DT) of ferrite from austenite above the  $A_{e3}$  during straining. Their simulations indicated that the two mechanisms could take place concurrently, with DRX being favored at the higher temperatures and lower strain rates, and DT being favored at the lower temperatures and higher strain rates. Sun *et al.* [5] in 2008 studied this phenomenon in some other low carbon steels and confirmed these observations. More recently at McGill, Jonas and co-workers [6] studied this behaviour in some low, medium and Nb-added microalloyed steels. There they found that the presence of Nb significantly delayed the reverse transformation.

This dynamic phenomenon cannot be predicted by the equilibrium phase diagram, but is expected to occur during the finishing stages of industrial hot rolling. Such dynamic transformations (under non-equilibrium conditions) lead to a decrease in the flow stress and therefore the rolling load. The decrease in flow stress after the peak results from the combined effects of DT and DRX. However, the parameters affecting this mechanism are not fully known at present and thus it has not been possible to control it in an industrially useful manner.

In all the above studies, the specimens were quenched in water to preserve the as-deformed high temperature microstructure. The conclusions are therefore based on samples examined after deformation had ceased. Questions have thus arisen about the possible occurrence of phase changes during the cooling interval. In order to distinguish with certainty between the dynamic and static phase changes, it is highly desirable to carry out in-situ experiments in which the phase changes are followed as they occur. The loading process should not be interrupted during the experiment. In fact it is extremely important to observe the phase changes during deformation. In-situ neutron diffraction is thus an ideal technique to study this phenomenon.

## EXPERIMENTAL DETAILS

In-situ neutron diffraction measurements were carried out in two different steels. Their chemical compositions and  $A_{e3}$  temperatures are given in **Table 1**. Investigations were done at temperatures above the  $A_{e3}$  during deformation. The samples were deformed in compression using a servo-hydraulic load frame in an Ar + 5% H<sub>2</sub> atmosphere to prevent oxidation of the steel. Cylindrical samples were tested using constant crosshead speeds. The transformation of austenite into ferrite was followed via the intensity variations of the ferrite {112} ( $\alpha_{112}$ ) peak. The peak was weak or non-existent at the start of the deformation step, so any increase in the ferrite signal can be attributed to the formation of ferrite during deformation.

**Table 1:** Chemical compositions (mass%) and  $Ae_3$  equilibrium transformation temperatures ( $^{\circ}C$ ) of the steels investigated.

Steel	C	Mn	Si	Nb	$Ae_3$ ( $^{\circ}C$ )
1	0.09	1.30	0.02	0.036	836
2	0.79	0.65	0.24	-	733

## RESULTS

Results from an in-situ compression test on the Nb-containing steel (Steel 1) are discussed here. A diffraction scan at  $876^{\circ}C$  is shown in Figure 1. The counting time per point was approximately 14 seconds. The average of all the readings is shown by the black horizontal line in the figure. The expected location of the ferrite (112) peak at this temperature is indicated by the vertical red line. Out of 36 measurements, 11 (31%) are further from the mean than one standard deviation. Thus the data show that no detectable ferrite (112) signal is present at this temperature prior to deformation.

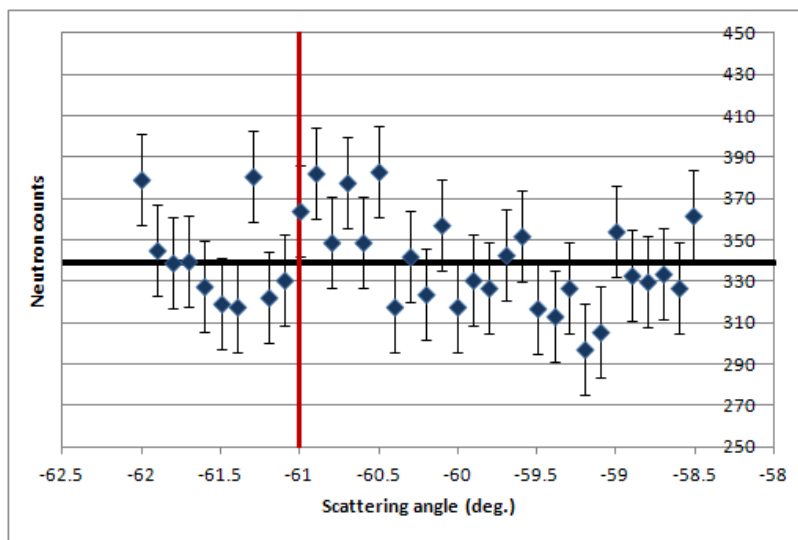


**Figure 1:** Diffraction scan at  $876^{\circ}C$  for sample Nb steel 9.

The sample was held at  $876^{\circ}C$  for approximately 20 minutes prior to starting the deformation step.

Figure 2 shows how the displacement of the upper compression rod and the neutron counts varied during the experiment. The neutron counting time for each measurement was  $\sim 1.47$  s. The crosshead moved at  $0.55$  mm/s during the test. As shown by the solid black line, the sample was compressed  $8$  mm (true strain of  $-0.663$ ) before being unloaded (see also the load-displacement curve in Figure 3). The global average of all the neutron data points is shown by the horizontal solid red line. The neutron counts did not change significantly

during the test: approximately 24% of the neutron data points in the graph deviate from the global average by more than one standard deviation. These data thus indicate that no ferrite formed during compression.

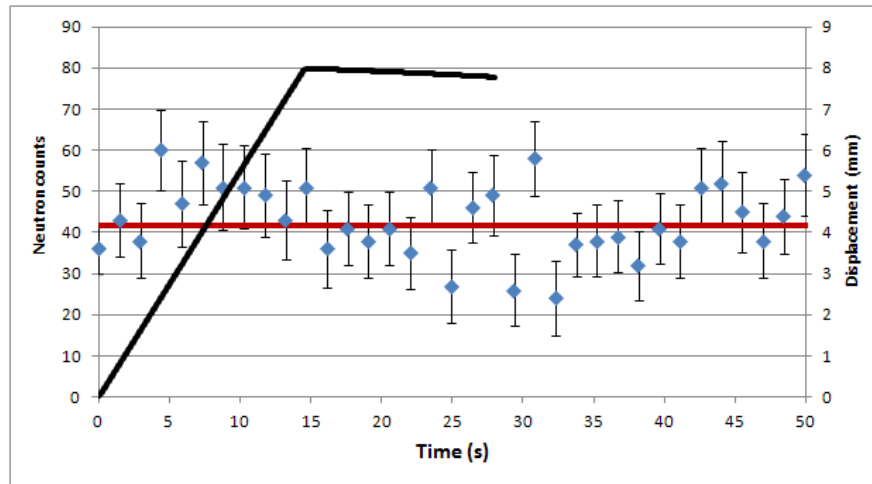


Figure 2: Variation of displacement and neutron counts.

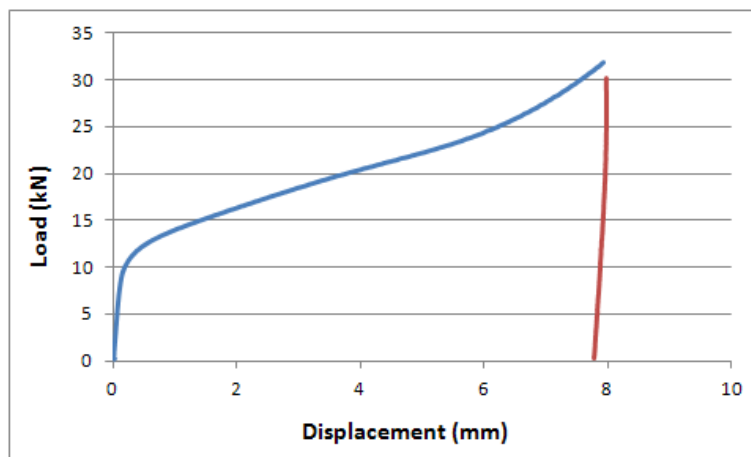


Figure 3: Load-displacement curve at 876°C.

## REFERENCES

1. Y. Matsumura and H. Yada: Trans. Iron Steel Inst. Jpn., 27 (1987), 492.
2. H. Yada, Y. Matsumura and T. Senuma: Proc. 1st Conf. Physical Metallurgy of Thermomechanical Processing of Steels and Other Metals (THERMEC-88), ed. by I. Tamura, ISIJ, Tokyo, (1988), 200.

3. M. Tong, J. Ni, Y. Zhang, D. Li and Y. Li: Metall. Mater. Trans. A, 35A (2004), 1565.
4. N. Xiao, D. Li and Y. Li: TMS, Supplemental Proc., Vol. 2, Materials Characterization, Computation and Modeling, (2009), 87.
5. X. Sun, H. Luo, H. Dong, Q. Liu and Y. Weng: ISIJ Int., 48 (2008), 994.
6. Vladimir V. Basabe and John J. Jonas: ISIJ International, 50 (2010), No. 8, 1185–1192.